Development of visual inspection system for low-reflective material utilizing of a string shadow

Keiji Kamei, Tomorou Kawahara
Department of Information Systems, School of Engineering, Nishinippon Institute of Technology
1-11 Aratsu, Kanda, Miyakogun, Fukuoka 800-0394, Japan

Yoshiyuki Daimaru
Nissan Motor Kyushu Co. Ltd., 1-3 Shinhama-cho, Kanda, Miyakogun, Fukuoka 800-0395, Japan
Email: kamei@nishitech.ac.jp

Abstract

Visual inspection of products in manufacturing plant is usually conducted by workers. However, that inspection process by workers occasionally happen oversight due to careless check, so that automatic visual inspection system is needed from manufacturer. Products made of low-reflective material are difficult to inspect by light reflection because contours of defect areas are got blurred. To solve this problem, we propose to inspect products utilizing of a string shadow. Form our research, a string shadow was different between contours of defect area and its of non-defect. On the other hand, former research did not success to detect defect area due to determination algorithm for defect. In this paper, we apply linear approximation of a string shadow to defect detection. From the experimental results, we succeed in detecting defects.

Keywords: Visual inspection system, low-reflective material, string shadow

1. Introduction

In the manufacturing industry, visual inspection in manufacturing plants is used to ensure the quality of products and parts. Most of the current visual inspections are performed by workers. However, visual inspection process by workers occasionally causes human errors such as variation in pass/fail criteria for defective parts or overlooking defective parts due to individual differences. For those reasons, demand for development of visual inspection system by image processing has been increased [1]. A template matching inspection method based on image recognition is an automated method of visual inspection [2], [3]. In inspection by template matching, the shape and location of the inspection target must be fixed. That method is an effective method if inspection items are simple and will not change significantly in the future. However, it is not suitable for the visual inspection system because it requires large cost when there are complex decisions, multiple types of inspection items or flexible responses to market trends.

In recent years, many studies has been conducted on product inspection systems that apply image recognition based on artificial intelligence(AI) [4]. In fact, we have been conducting research on image recognizers using artificial intelligence in our research [5]. However, AI-based product inspection systems cannot explain the reasons for wrong decisions due to the problem of the AI being a black box [6], [7]. So, this research does not apply AI for visual inspection system.

This research aims to construct a visual inspection system that can detect defects whose position is not fixed and whose shape is unknown. In general, such visual inspections detect defects based on the reflection of linear light such as fluorescent lights. On the other hand, this study targets the products made of low-reflective materials which do not reflect lights; so that, our visual inspection system is not able to use reflection of lights. To overcome this difficulty, we propose to utilize a string shadow to detect defective area. The shadow of string has the property of changing shape based on distortion of the material when projected onto low-reflective materials. Our method uses this property to detect distortion of low-reflective materials based on the shadow shape of string. In this research, our method can flexibly detect by characterizing the defective area utilizing a string shadow and determination the defective area not by pattern matching but by the distance to the approximate linear line of a string shadow. From the experimental results, we succeed in detecting defects on material.

2. Method for defective detection

We introduce the method of defective detection utilizing a string shadow in this section.

2.1. *Characterization from a string shadow*

Out method for visual inspection is to light on a string that placed horizontally to the inspection target and to form a string shadow on it, then that judges defective or non-defective from form of a string shadow. Fig. 1(a)

shows the shadow of a non-defective material and (b) the shadow of a defective material.

For preprocessing, the shadow image from the camera is denoised by Gaussian filter, binarized, and then edge-smoothed again by Gaussian filter by OpenCV [8] as shown in Fig. 2.

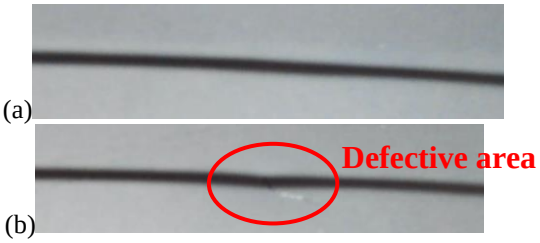

Fig.1 String shadow. (a)non-defective. (b)defective.

Fig.2 Example of after preprocessing.

2.2. *Environment for inspection*

The string shadow is affected by positions for light, camera, string and material as follows.

1. The closer the distance between light and a string, the more the light diffuses and a shadow becomes more fading.
2. The closer the distance between a string and the material, the darker the shadow of a string.
3. When the distance between light and a string is about 45 cm, light is not diffused and shadow is clearly projected.
4. The smaller the angle between the camera and the material, larger the change in the shape of the shadow of the defective area.

From these features for a string shadow, the positional relationship is chosen to have the largest change in the shape of shadow of defective area, as shown in Fig. 3.

2.3. *Linear approximation of a string shadow and judgement based on sum of distance between line and shadow*

Fig. 4 shows that area of non-defective shadow has an almost constant gradient, whereas one part of gradient changes for the defective one. When the contour on the upper side of shadow is approximated by linear line,

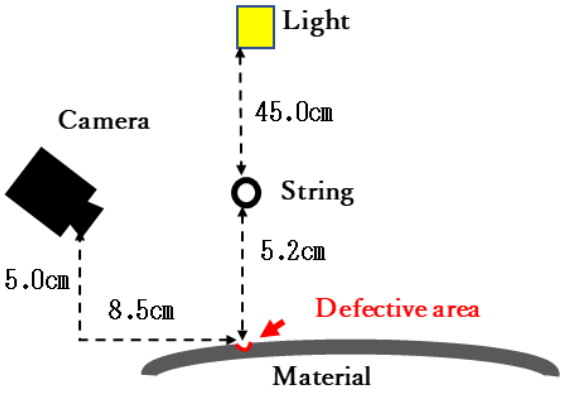

Fig.3 Positional relationship.

defect detection is based on the sum of relative distances between shadow and approximated linear line.

Fig.4 Defective shadow after preprocessing.

When width of linear approximation is Δy, the examples of linear approximated line by start point y and end point $y + \Delta y$ are shown in Fig. 5. A wide black area is created between approximated linear line and shadow contour in defective case as Fig. 5(b).

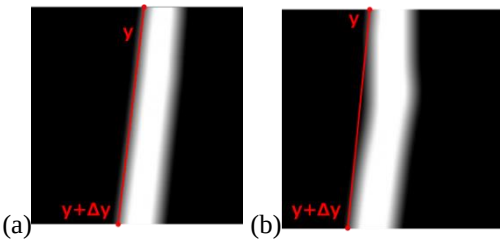

Fig.5 Differences of shadow. (a)non-defective. (b)defective

When the approximated linear line is $f(y)$ and the shadow curve is $g(y)$, gradient a of the approximated linear line is Eq. (1). Thus, linear line, $f(y)$, approximated equation is Eq. (2).

$$a = \frac{g(y_0+\Delta y)-g(y_0)}{\Delta y} \quad (1)$$

$$f(y) = y_0 + a(y - y_0) \quad (2)$$

where, y_0 is start point of linear line. The sum of relative distances between shadow and approximated linear line is defined as,

$$S = \int_y^{y+\Delta y} |f(y) - g(y)| dy \quad (3)$$

S in Eq. (3) in defective case is larger than non-defective case from Fig. 5. S is obtained by shifting the starting point, then the sum of S is used to determine non-defective and defective. Since this method makes relative

judgments rather than absolute judgments, it is expected to have a high degree of flexibility to suit a wide variety of shapes. On the other hand, a problem with this method is the possibility of successfully approximating the defect area as a linear line depending on the value of Δy. To solve this problem, starting point y for approximated linear line is shifted several times to vary the sum of the relative distances, then determination of non-defects and defects is based on comprehensive results. This will avoid inspection errors by considering approximations which are not coincidental successes of linear line approximations.

3. Experiments

We first examine the variation of shadow contour with and without defects, and then examine the difference in the sum of relative distances between approximated linear line and a shadow contour with and without defects.

3.1. *Sample of visual inspection*

Fig. 6 shows the non-defective and defective samples used to be inspected. The defective sample has two kinds of defectives with different concavities, i.e., dent and depression.

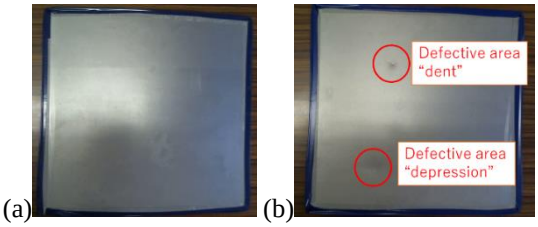

(a) (b)

Fig.6 Samples. (a)non-defective. (b)defective

3.2. *Comparison of shadow contour*

Fig. 7 shows the variations in shadow contour coordinates with and without a dent defect. The figure shows that gradient varies linearly without dent, while gradient with dent varies significantly around y at 500 to 700, which is the defective area, in the case of dent defect.

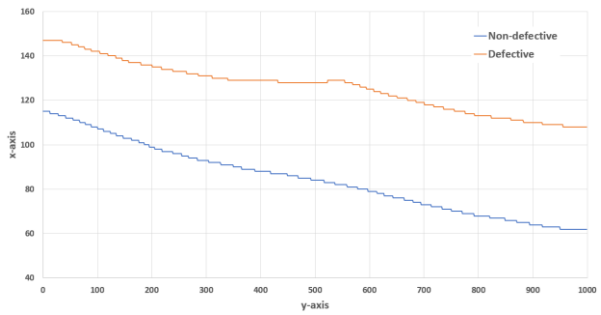

Fig.7 Comparison results of shadow contour(dent)

The same variations are also observed in case of depression. From these results, it can be said that the shadow contours are characterized by a large gradient variation in the defective area.

The product to be inspected in this study does not have a horizontal surface when viewed from the side. In addition, because the height varies depending on the inspection location, the shape of shadow and the location where it is formed are continuously altered. A method of determining by the rate of change of gradient could be considered, but it is difficult to define determination sections because gradient varies depending on the inspection location and the shape of the product and size of defect.

3.3. *Defect detection based on the sum of relative distances between a string shadow and linear line approximation*

In this experiment, two non-defective shadow images are utilized for each defect, shown as Fig. 8(a), to also verify the sum of the relative distances of non-defective shadows, shown as red and green area in Fig. 8(b).

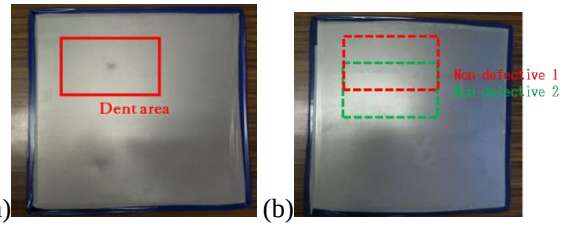

(a) (b)

Fig.8 Example of viewpoint. (a)dent defective. (b)non-defective

The results of linear line approximation of dent defect and non-defect are shown in Fig. 9 with the starting point of approximation set to 0 and Δy set to 200. Fig. 10 shows the actual coordinates of a string shadow.

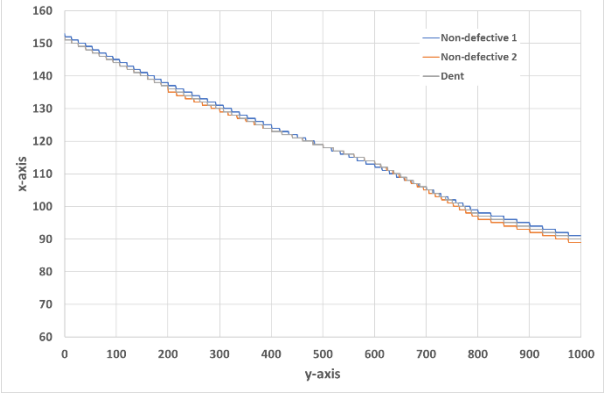

Fig.9 Liner line approx. for "Dent defect"

From figures, there is a large deviation between the approximated linear line and the actual coordinates for defect and non-defects with y-axis between 500 and 600. The same deviation is also happened in case of depression.

Table 1 shows the results of comparison for the sum of relative distances between a string shadow and linear line approximation in case of dent and depression defects.

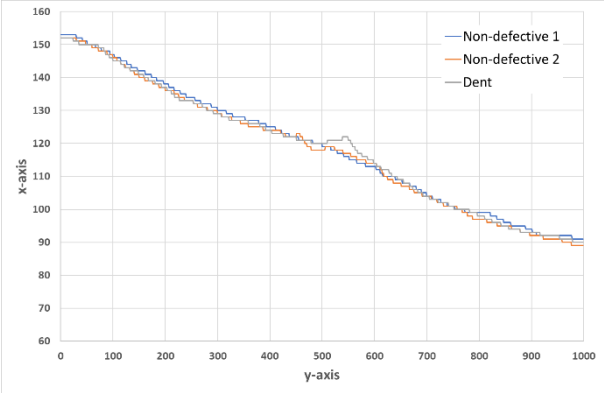

Fig.10 Before liner line approx. for "Dent defect"

Table 1. Comparison of the sum of relative dist.

	Kind of defect	Non-defect1	Non-defect2	defect
Sum of relative dist.	dent	340	344	668
	depression	458	394	576

Table 1 shows that the sum of relative distance with dent is about 300 larger than without, and about 150 larger for depression. It can be said that the sum of relative distances is smaller because of the gradual change in shadow in case of depression defect. For this, it is shown that linear line approximation successfully for slowly varying defects and might fail to detect defects. To solve this, starting point y for approximated linear line is shifted, mentioned in Section 2.3. Let d be the distance of the start point y from the image origin and shift y 19 times in total by +10 in the range of $d = 0$ to 190, then obtain the sum of relative distances for 20 times. Table 2 shows the results of shifting of starting point.

Table 2. Results of shifting. ND1, ND2 and Df correspond to "Non-defective 1", "Non-defective 2" and "defective", respectively.

	dent			depression		
	ND1	ND2	Df	ND1	ND2	Df
Avg.	448.5	459.4	582.3	406.0	399.3	565.4
Max	653	696	881	662	546	828
Min	304	271	435	234	252	341

Table 2 shows that the mean, maximum, and minimum values differ by about 100 or more between the undistorted and the distorted samples. In particular, it can be said that defects in products can be detected by using the maximum value as a criterion for determination because the maximum value differs by about 200 depending on occurrence of defects. From these results, defect detection can be performed flexibly for defect detection problems that cannot be solved by template matching.

4. Discussions

Real-time processing is required in the production environment, and the camera frame rate is 30 fps, so processing must be completed within 33[ms] before the next image is received. The frame rate at 200[kpx] is 20[ms], on the other hand, at 900[kpx] of it is 55[ms]; consequently, a frame rate drop occurred. So, it can be expected that current PC can support up to about 500[kpx], otherwise stronger PC is needed.

5. Conclusions

In this study, defect images are characterized by the shadow of a string to develop a defect detection method for low-reflective materials, and defect features are detected not by pattern matching but by the sum of relative distances to an approximated linear line. From the experiment, it is effective to shift the starting position multiple times because the sum of relative distance varies greatly depending on the starting position of the approximated linear line. It can also be said that defect detection is possible by using the maximum value as a defect determination criterion. We aim to further improve the system by conducting experiments in actual environments and trying out various kinds of samples.

Acknowledgements

This work was supported by NISSAN Motor Kyushu Co., Ltd, Japan. We also appreciate Nissan Motor Kyushu Co., Ltd. for providing various test samples, computers, cameras, lights, and other equipment.

References

1. Newman, Timothy S., and Anil K. Jain. "A survey of automated visual inspection," Computer vision and image understanding 61.2 (1995): 231-262.
2. Brunelli, Roberto. "Template matching techniques in computer vision: theory and practice," John Wiley & Sons, 2009.
3. Kamei, Keiji and Moriyama, Hiroyuki, "Recognition Method of Target Objects for Autonomous Tomato Harvesting Robot," Proc. 2019 Int. Conf. on Artificial Life and Robotics, (ICAROB2019), pp.557-560.
4. Huang, Szu-Hao, and Ying-Cheng Pan. "Automated visual inspection in the semiconductor industry: A survey," Computers in industry 66 (2015): 1-10.
5. Kamei, Keiji, et al. "Development of the Image-based Flight and Tree Measurement System in a Forest using a Drone," J. Robotics Netw. Artif. Life 7.2 (2020): 86-90.
6. Hachiya, Tatsuma and Kamei, Keiji. "Factor identification and prediction of power demand using sparse modeling AI," Proc. the 12th Int. Conf. on Innovative Computing, Information and Control, (ICICIC, 2023), pp. 71.
7. DARPA. "Special Issue:DARPA's Explainable Artificial Intelligence (XAI) Program," APPLIED AI LETTERS, Vol.2, Issure 4, 2021.
8. Adrian Kaehler and Gary Bradski. "Learning OpenCV 3," O'Reilly Media, Inc., 2016.

Authors Introduction

Dr. Keiji Kamei

In 2007 he obtained his PhD at the Department of Brain Science and Engineering, Kyushu Institute of Technology (Engineering). From April, 2007 to March, 2014, he was a lecturer, and from April, 2014 to March 2020, he was an associate professor. April, 2020, he has been a professor, Nishinippon Institute of Technology. His research interests are Artificial Neural Networks, Artificial Intelligence, Artificial Life and Computer Science. A member of JNNS, APNNS, IPSJ, IEICE, SOFT.

Mr. Tomorou Kawahara

He is a bachelor research member in Kamei laboratory at Nishinippon Institute of Technology. His research interest is image processing.

Mr. Yoshiyuki Daimaru

He is an employee of Nissan Motor Kyushu Co. Ltd. and a co-researcher on the corporate side of this research.